EDGEWOOD

CHEMICAL BIOLOGICAL CENTER

U.S. ARMY RESEARCH, DEVELOPMENT AND ENGINEERING COMMAND

ECBC-TR-352

DETECTING CHEMICAL AND BIOLOGICAL MUNITIONS USING INFRARED IMAGING SYSTEMS, ADVANCED IMAGE PROCESSING AND FEATURE EXTRACTION METHODS, AND LINGUISTIC-FUZZY CLASSIFIERS

Bruce N. Nelson

GEO-CENTERS, INC.
Newton Centre, MA 02459

Amnon Birenzvige

RESEARCH AND TECHNOLOGY DIRECTORATE

July 2004

ABERDEEN PROVING GROUND, MD 21010-5424

Disclaimer

The findings in this report are not to be construed as an official Department of the Army position unless so designated by other authorizing documents.

REPORT DOCUMENTATION PAGE

Form Approved
OMB No. 0704-0188

1. REPORT DATE *(DD-MM-YYYY)*	2. REPORT TYPE	3. DATES COVERED *(From - To)*
XX-07-2004	Final	Aug 2001 - Jul 2003

4. TITLE AND SUBTITLE
Detecting Chemical and Biological Munitions Using Infrared Imaging Systems, Advanced Image Processing and Feature Extraction Methods, and Linguistic-Fuzzy Classifiers

5a. CONTRACT NUMBER

5b. GRANT NUMBER

5c. PROGRAM ELEMENT NUMBER

6. AUTHOR(S)
Nelson, Bruce, N.; (GEO-CENTERS, INC.); and Birenzvige, Amnon (ECBC)

5d. PROJECT NUMBER
206023.84BPO

5e. TASK NUMBER

5f. WORK UNIT NUMBER

7. PERFORMING ORGANIZATION NAME(S) AND ADDRESS(ES) AND ADDRESS(ES)
GEO-CENTERS, INC., 7 Wells Avenue, Newton Centre, MA 02459
DIR, ECBC, ATTN: AMSRD-ECB-RT-II, APG, MD 21010-5424

8. PERFORMING ORGANIZATION REPORT NUMBER
ECBC-TR-352

9. SPONSORING / MONITORING AGENCY NAME(S) AND ADDRESS(ES)

10. SPONSOR/MONITOR'S ACRONYM(S)

11. SPONSOR/MONITOR'S REPORT NUMBER(S)

12. DISTRIBUTION / AVAILABILITY STATEMENT
Approved for public release; distribution is unlimited.

13. SUPPLEMENTARY NOTES

14. ABSTRACT

This report is one in a series of reports describing the Disparate Sensor Integration (DSI) program. The purpose of the program is to determine if employment of CB weapons can be detected by existing (non-CB) sensors in a dual use mode. Specifically, this report describes how an existing Air Force IR imager can successfully discriminate between HE and CB artillery rounds during detonation. The report also describes how a newly developed data fusion technique, the Liguistic Fuzzy Logic, can be used to fuse together several discriminating features of the IR images to achieve this discrimination with a high degree of reliability. The reliability of the discrimination exceeds 90%. In addition, we are able to determine if the CB round detonated in the air or upon ground impact. This information is important for estimating the footprint of the chemical/biological plume.

15. SUBJECT TERMS

Disparate sensors	Data fusion	CB early warning
IR imager	Discriminating algorithm	Fuzzy logic
Chemical/Biological weapons	CB detection	

16. SECURITY CLASSIFICATION OF:			17. LIMITATION OF ABSTRACT	18. NUMBER OF PAGES	19a. NAME OF RESPONSIBLE PERSON
a. REPORT	b. ABSTRACT	c. THIS PAGE			Sandra J. Johnson
U	U	U	UL	33	19b. TELEPHONE NUMBER *(include area code)* (410) 436-2914

Blank

PREFACE

The work described in this report was authorized under Project No. 206023.84BPO. This work was started in August 2001 and completed in July 2003.

The use of either trade or manufacturers' names in this report does not constitute an official endorsement of any commercial products. This report may not be cited for purposes of advertisement.

The report has been approved for public release. Registered users should request additional copies from the Defense Technical Information Center; unregistered users should direct such requests to the National Technical Information Service.

Blank

CONTENTS

FIGURES

TABLES

DETECTING CHEMICAL AND BIOLOGICAL MUNITIONS USING INFRARED IMAGING SYSTEMS, ADVANCED IMAGE PROCESSING AND FEATURE EXTRACTION METHODS, AND LINGUISTIC-FUZZY CLASSIFIERS

1. INTRODUCTION

In September 2001, the U.S. Army Edgewood Chemical Biological Center (ECBC) conducted a field test at Dugway Proving Ground (DPG), Dugway, UT. The test was part of the Disparate Sensor Integration (DSI) program. The purpose of the program is to determine if chemical/biological (CB) munitions could be detected, based on their different signatures during detonation. During the test, 260 155mm artillery rounds were fired. The classes of 160 of these munitions were known to the analyst and were used to help identify critical features and develop algorithms to detect CB munitions. The last 100 rounds were blind (to the analyst) and were used to test the robustness of the discriminating algorithms. The rounds were divided equally between conventional (HE) and simulated CB rounds. The conventional rounds contained 15 lb of high explosive (HE), while the CB rounds contained about 1.5 lb of HE and were filled with a 50-50% mixture of water and poly ethylene glycol. Half of the munitions were fused to detonate upon ground impact. The other half were fused for airburst. The rounds were fired in random order. Detailed descriptions of the test and the various sensors used are given in ECBC-TR-251.[1]

In support of the DSI Program, several camera systems were fielded to determine the feasibility of using information from these systems to discriminate between chemical and conventional munitions. The cameras fielded included two visible wavelength cameras, a near infrared (IR) camera (peak response at approximately 1 μm), a mid wavelength IR camera system (3 μm - 5 μm), and three long wavelength IR camera systems (7.5 μm - 13 μm).

One of these imaging systems was a U.S. Air Force-deployed system currently used for surveillance on the battlefield. The Long Wavelength IR Imaging System uses an un-cooled silicon microbolimeter (320 x 240 pixels) detector array that is sensitive over the 7.5 - 13 μm spectral range. This system is relatively inexpensive compared to other imaging sensors evaluated. More importantly, it is a fielded system that is currently used on the battlefield. Other reports[2,3] summarized the results from preliminary work performed on data generated from this and a visible spectral range imaging system. These reports describe some basic features with potential use in discriminating between the different classes of munitions' detonation events. This work also demonstrated the potential for achieving this discrimination within approximately 1/3 of a second (10 frames) from detonation time.

This report describes some of the more recent work performed on the DSI Air Force IR imaging system data set. Specifically, this report will first detail the "detector" used to identify munitions' detonation events within detonation video sequences and will provide representative imagery from each of the four classes of munitions detonations (HE point detonation, CB point detonation, HE airburst, and CB airburst). This information will be followed by descriptions of the features extracted from frames of interest within the video sequence. Conversion of the features extracted from individual frames to a final feature vector (used as input to a classification system) will then be described. The linguistic-fuzzy classifiers[4]

used to analyze this feature vector and to estimate munition's detonation event class confidence will be described in detail. A discussion of the results obtained on the DSI training and blind data sets using the previously described methodologies will follow. The report will conclude with recommendations and discussions on how the confidence values generated and feature values can be used to support DSI sensor and data fusion activities.

2. DETECTOR DESCRIPTION AND REPRESENTATIVE IMAGERY

This section of the report will first describe the detector used to identify "frames" of interest in the DSI video sequences. This will be followed by representative imagery from each of the four classes of events:

(1) CB airburst
(2) HE airburst
(3) CB ground detonation
(4) HE ground detonation

The DSI imaging sensor data were archived and made available to DSI team members as AVI files (compressed with various CODECs). These files typically consist of a video sequence with some background video followed by the munition's detonation event followed by some additional background video. The events of interest last between 3 and 100 (or more) frames within these sequences. Consequently, we wanted to develop a detector that could be used to isolate and identify frames of interest within the video sequence. This detector is described in detail in the following paragraphs. It will become apparent in following discussions that a secondary benefit of this detector is that in the image, it also identifies the specific pixel locations associated with the munition's detonation event.

Figure 1 provides a representative frame extracted from the 3rd frame after detonation from an HE airburst. This frame is converted to a digital grayscale image whose intensity varies from 0 (dark or "hot") to 1 (light or "cold") using MATLAB. The munition's detonation event is clearly observable in the image as the dark object in the upper right section of Figure 1.

A "change" image is first created by subtracting the frame captured 20 frames (~2/3 s) earlier from the frame being analyzed. As the intensities of each of these frames varies between 0 and 1, the change image will vary between –1 (for dark or "hot" objects) to +1 (for light or "cold" objects). The result of performing this operation is shown in Figure 2. This change detector generates an image with a relatively neutral background (gray) with one large dark (hot) object directly associated with the detonation event.

Next, we perform what we call adaptive thresholding of the change image to create a binary image. Adaptive thresholding is required in this application to ensure that detonation events are properly identified in the binary image. This requirement stems from the wide variability in intensity values as well as other video attributes of the munitions' detonation signatures. The imagery shown later in this section of the report further illustrates this point.

Figure 1. Image Associated with the 3rd Frame After an HE Airburst

Figure 2. Change Image Generated from the Image Previously Shown in Figure 1

We have used the following adaptive threshold process:

- Calculate the standard deviation of each column in the digitized form of the change image.

- Calculate the median of these standard deviation values. This value indicates the "noise level" in the background section of the image. This is because the detonation signature occurs over only a few columns (compared to the total number of columns) in the change image.

- Since the detonation image always appears to be darker (hotter), we apply a threshold to identify darker objects in the change image. Specifically, we will look for signatures that are darker by nine standard deviations than the background noise level in the image. The value nine was chosen since it appears to consistently highlight detonation signatures of interest in the video sequences.

- We perform the following operation to create the binary image using the techniques described above.

BinImage = Change Image < - 9 * [median(change image column standard deviations)]

This operation sets all pixel values less than the indicated threshold to 1 and all pixel values greater than or equal to this threshold value to 0.

The result of performing the above process on the image previously shown in Figure 2 is shown in Figure 3. The "on pixels" in the binary image (Figure 3) directly correspond to the detonation event signature. The imagery shown later in this section of the report further illustrates the ability of these methods to identify the detonation signature in video sequences. Note that the detector used in support of the work performed in References 2 and 3 uses the same process (with one minor exception - it also looks for light objects) as described above. This technique has allowed us to reliably detect detonation sequences in video sequences regardless of the detonation signature intensity levels and the background against which the event occurs.

Figure 3. Binary Image Generated from the Change Image Previously Shown in Figure 2

Now, we perform a morphological operation on the binary image. This process removes all objects ≤ 3 pixels in size. In the case shown in Figure 3, there are no objects smaller than 3 pixels. Consequently, this operation does not alter this binary image.

The final step is to determine the total number of "on" pixels in the binary image. If the total number of "on" pixels is more than 3, the detector is considered "triggered." Otherwise, the frame being analyzed is not considered a frame of interest. The value of 3 pixels is selected as it consistently affords the detection of signals of interest without a significant number of false alarms. This same threshold has been used on the DSI visible (at two focal length settings) and IR camera data.

The classifier described later in this report works with up to four frames (total) from a video sequence. Each time the detector triggers, the frame number as well as extracted features are written to a file. When the first frame is detected, the detonation video sequence starts. We examine 10 frames in the detonation sequence and extract features from the first frame on which the detector triggers. We also try to extract features from the 2^{nd}, 3^{rd}, and 10^{th} frames in the detonation video sequence. If the detector is not triggered on these frames, we extract features from the first 2 frames on which the detector triggers (or from less frames if the detector does not trigger two additional times during the first 10 frames of the detonation sequence). We always try to extract features from the 10^{th} frame in the detonation video sequence. When working with this last frame, features are extracted only if the detector triggers on this video frame. In general, for strong munition detonation signals, the detector will trigger, and features will be extracted from the 1^{st}, 2^{nd}, 3^{rd}, and 10^{th} frames after a munition's detonation. When the signatures are less strong, the detector may only trigger on (and features will be extracted from) either the first three frames after detonation, or the 1^{st}, 3^{rd}, 5^{th}, and 10^{th} frames or just on the 1^{st} and 2^{nd} frames. There are many possibilities for how the detector will trigger during a particular video sequence, and that the specifics of its triggering are generally driven by the specific characteristics of a munition's detonation signature. Our experience has been that in the majority of cases where the detector does not trigger on all frames (or triggers on frames other than the 1^{st}, 2^{nd}, 3^{rd}, and 10^{th} frames) that the detector still generally only triggers on a munition's detonation signals. This is a direct result of the adaptive thresholding methods and the 3-pixel threshold used in this detector.

The following figures and paragraphs will provide images extracted from the video sequences for each of the four classes of munitions' detonation events. In all of the figures, the images on the left are extracted directly from the video sequence. The images on the right are the binary images generated from the images on the left using methodologies described above. In all of the figures, the top images are from an HE airburst. The second row of images is from a CB airburst. The third row of images is from an HE point detonation, and the final row of images is from a CB point detonation.

Figure 4, 5, 6, and 7 provide the images generated for the four classes of munitions' detonation events for the 1^{st}, 2^{nd}, 3^{rd}, and 10^{th} frames after munitions' detonations, respectively. These figures are discussed in more detail in Section 3, which describes the features used for discriminating between CB and HE events. These features are extracted from these four video frames. We discuss how these features are reduced to a final feature vector for each munition's detonation event. This feature vector becomes the input to the classification system described in detail later in this report.

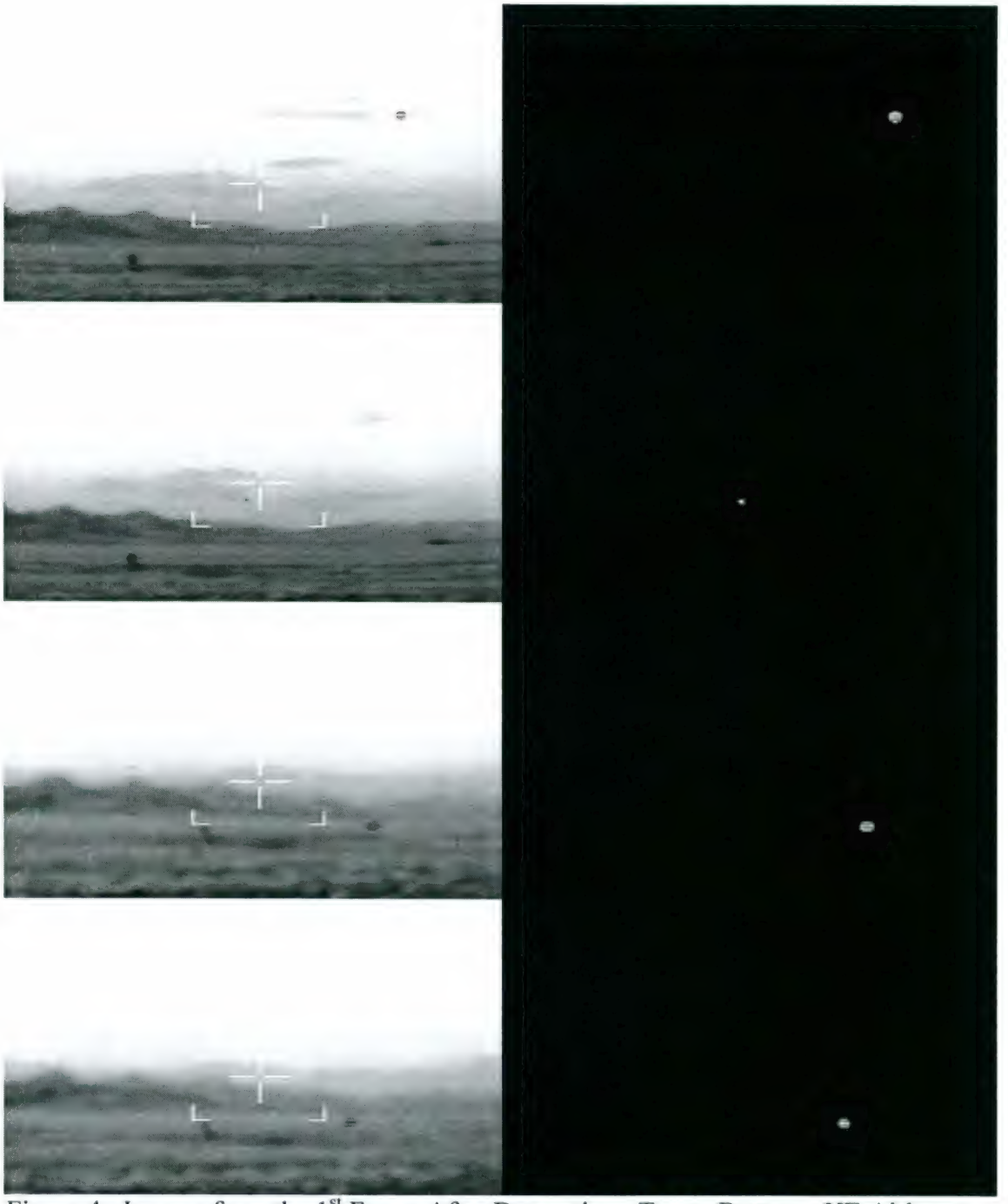

Figure 4. Images from the 1st Frame After Detonation. Top to Bottom: HE Airburst, CB Airburst, HE Point Detonation, and CB Point Detonation

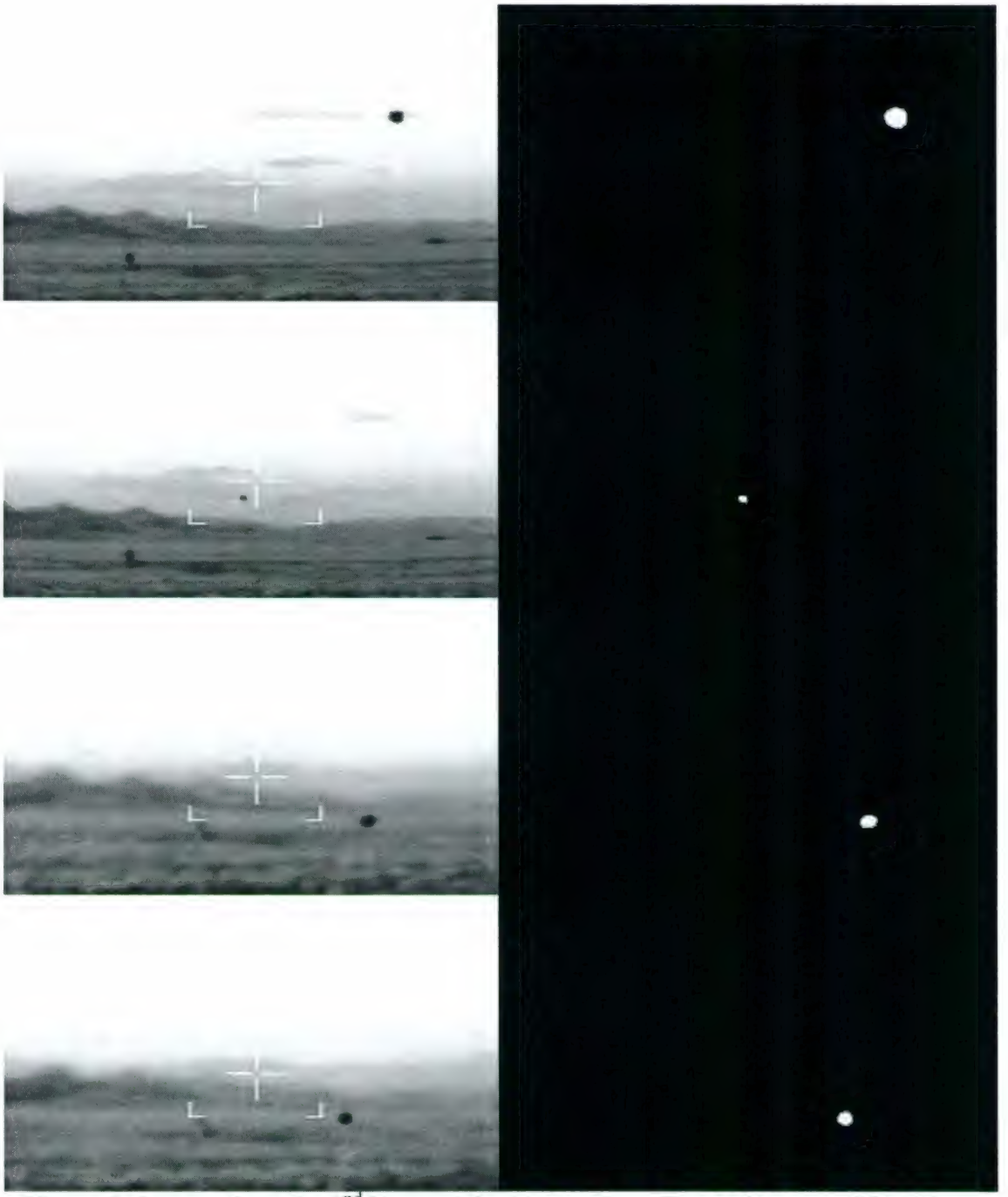

Figure 5. Images from the 2nd Frame After Detonation. Top to Bottom: HE Airburst, CB Airburst, HE Point Detonation, and CB Point Detonation

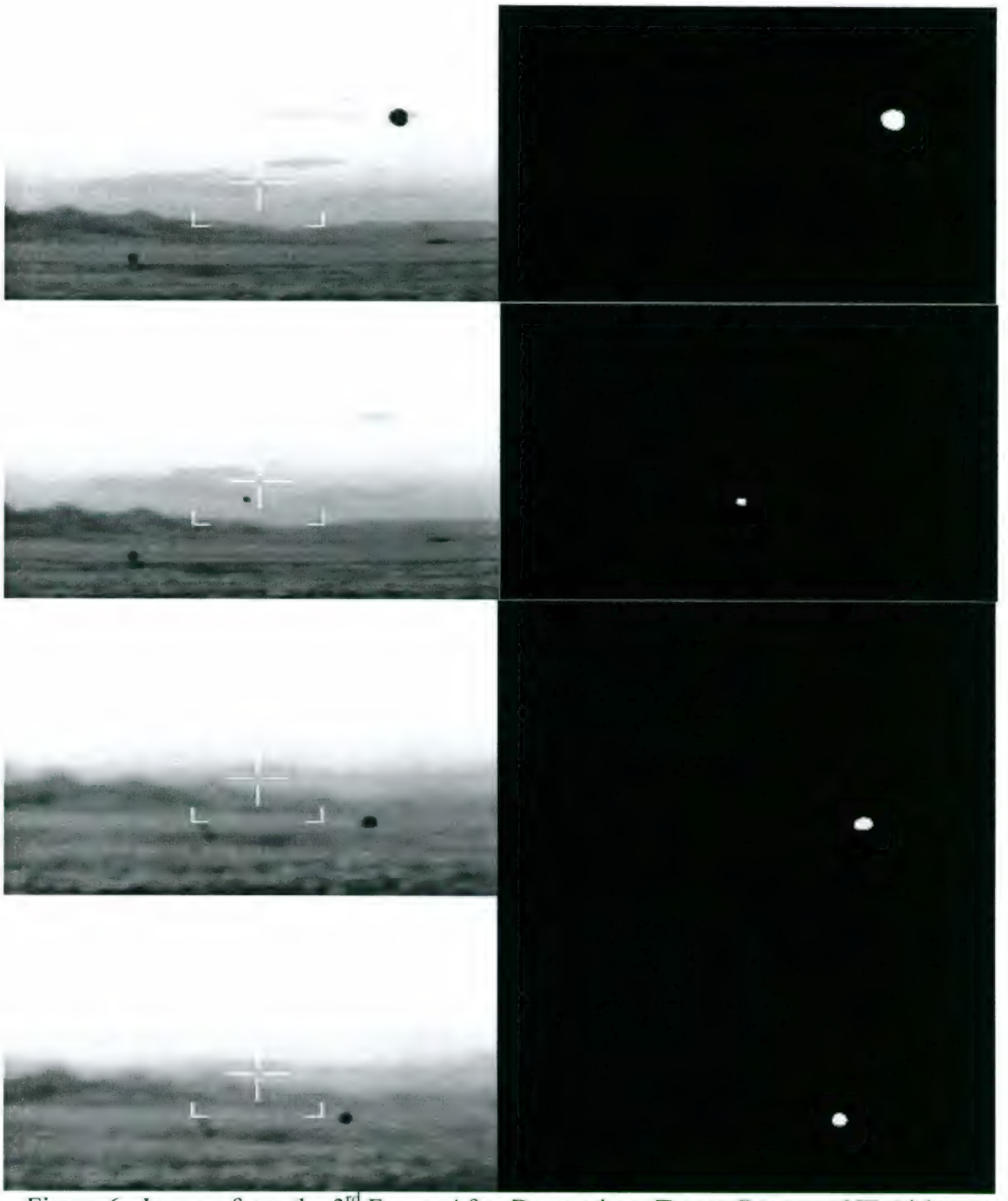

Figure 6. Images from the 3rd Frame After Detonation. Top to Bottom: HE Airburst, CB Airburst, HE Point Detonation, and CB Point Detonation

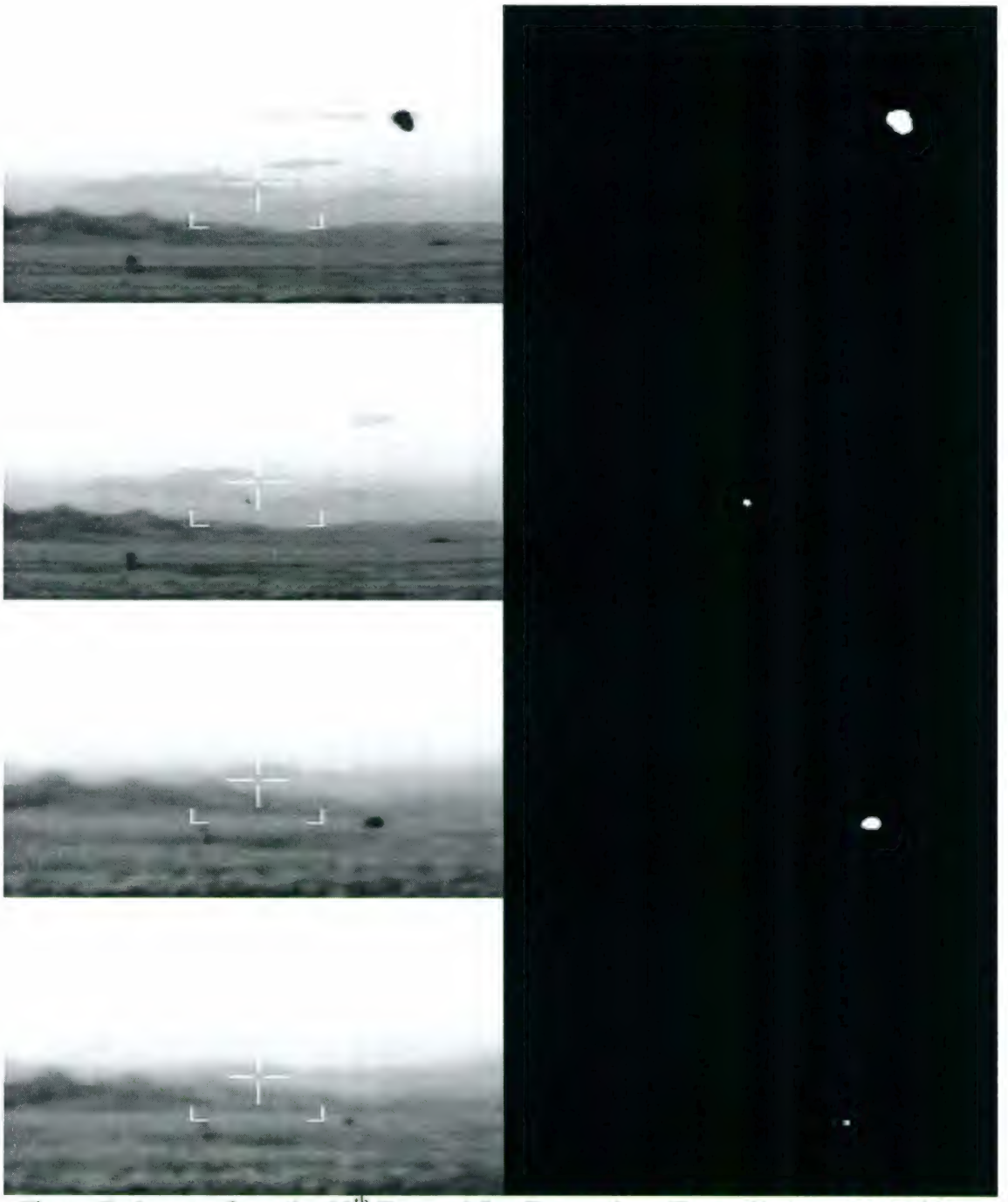

Figure 7. Images from the 10th Frame After Detonation. Top to Bottom: HE Airburst, CB Airburst, HE Point Detonation, and CB Point Detonation

3. FEATURE EXTRACTION AND FEATURE VECTOR DEVELOPMENT

Each time the detector "triggers" on a video frame, a set of features are extracted from that frame. The features from up to four frames are reduced to a single feature vector. This vector is used in a classifier described in Section 4 of this report. This section will describe the specific features extracted from each video frame and will also describe how the information from the video frames (up to four) are condensed to create a single feature vector. Section 4 will also provide an overview of how this vector is used in discriminating between the different classes of munitions' detonations. Section 4 will also describe in detail the classifier that acts on the feature vector and will provide the results of applying this classifier to the AF IR video imagery collected during the DSI field trial.

When the detector is triggered (by a frame of interest), the binary image is labeled. In cases where there is only a single object in the binary image, features are extracted from the labeled blob. The features are extracted for each blob in the image in cases where there are more than one blob labeled in the binary image. The following paragraphs describe the features that are currently extracted from the frames of interest (up to four) in the AF IR video data.

A review of the information shown in Figure 7 clearly shows that detonations of CB munitions result in objects of much smaller size in the 10^{th} frame after a munition's detonation compared to those for HE munitions. Consequently, the size of objects in the binary images provides a good feature for discriminating between CB and HE munitions. Figure 7 also shows two other points. First, there is an orientation of blobs in the binary image associated with the HE air detonations that is consistent with the azimuth of the incoming round and that the signal-to-noise ratio of the CB signatures is significantly smaller than that of the HE signatures. This latter observation results either in the detector not triggering in sequence or in the detector not triggering four times when working with CB-generated video sequences. A review of the data shown in Figures 5, 6, and 7 shows that the eccentricity is higher (i.e., the blob is more elliptical) in HE point and air detonations when compared to the CB point and air detonations.

Features are extracted from frames of interest in each video segment. Features extracted from the video segments used for discrimination are the size of objects, the orientation and the eccentricity of blobs, and whether or not the detector triggered sequentially when it ran on a particular video segment. Features based on the grayscale levels associated with objects identified in the binary image and on the rate of change of the size of objects in the binary image between frames were also evaluated. However, these latter features are not currently used in performing CB round discrimination as they did not provide sufficient new information for detonation event classification.

The first feature we extract from the video frames of interest is the size (number of "on" pixels) of objects in the binary image. Primarily, it is this feature that is used to discriminate between CB and HE munition detonations.

Next, we extract the orientation of the blobs in the binary image. To accomplish this, we render the blob as an ellipse and compute the ellipses major and minor axes. The blob orientation feature is the orientation of the major axis with respect to the horizontal axis. In

cases where there are multiple blobs within an image's frame, the minimum angular orientation of the different blobs is used as the orientation feature for the frame being analyzed. Improved classification performance is likely with an improved means of extracting this feature when there are multiple blobs within an image frame.

Next, we extract an eccentricity feature from the blobs in the binary image. The eccentricity is the ratio of the ellipse major axis and is determined by first rendering the blob as an ellipse. Consequently, an object with an eccentricity of 0 is circular, and an object with an eccentricity of 1 is a line. In cases where there are multiple blobs present in a frame of interest, we average the values of the eccentricities of all the blobs present in the image and use that value as the eccentricity feature. Again, improved classification performance is likely with an improved means of extracting this feature in cases where there are multiple blobs within an image frame.

When the detector triggers, the test number (extracted from the file name), frame number, and each of the features described above are written to a file. Table 1 provides an example of such information, in this case for an HE airburst event.

Table 1. Extracted Features from an HE Airburst Munition Detonation

Test Name	Frame Number	Number of "On" Pixels	Blob Orientation	Blob Eccentricity
T258 (#21)	81	107	0	0.99
T258 (#21)	82	400	-1.55	0.88
T258 (#21)	83	638	-12.84	0.47
T258 (#21)	90	794	-42.47	0.62
4				

The number 4 at the bottom of the table indicates that the detector fired for each of the four frames being analyzed. As previously discussed, in some cases, the detector either triggers on less than four frames or does not trigger on the 1st, 2nd, 3rd, and 10th frames after detonation. This occurs most often for CB detonations and is generally a result of the lower signal-to-noise ratio for this type signature for this class of munitions' detonations. In all cases, features such as those presented in Table 1 are combined to create a single feature vector for the particular video segment being analyzed. It is this final feature vector that is used as input to the classifiers described in Section 4.

The following steps describe how the features are combined:

a. Set the size1 feature value to the number of "on" (non-zero) pixels in the last frame on which the detector triggered. (Note that this last frame can be any frame within the first 10 frames after a munition's detonation. When the detector triggers four times, this information will always be the 10th frame. In other cases, the last frame can be any frame within the first 10 frames. It is the specifics of a given video segment that determine which frame this will be).

b. Set the Orientation Feature to the value associated with the 10^{th} frame after detonation (fourth row of Table 1). In cases where the detector triggers less than four times, the Orientation Feature is set to zero.

c. Set the eccentricity to the average of the eccentricity values extracted from the 2^{nd} and 3^{rd} frames following a munition's detonation. In cases where there are multiple blobs present in these two frames, the eccentricity feature value generated from that frame is not considered. In such cases, the eccentricity value is the eccentricity value extracted from the frame where there is only one object present. In cases where both of these frames have more than one object, the eccentricity value is set to 0.

d. Declare an event sequential when the detector triggers on the 1^{st}, 2^{nd}, 3^{rd}, and 10^{th} frames. Declare an event as nonsequential when this is not the case.

Table 2. Final Feature Vector Generated from Table 1 Data

Test Name	Size1	Orientation	Eccentricity	Sequential
T258 (#21)	794	-42.47	0.545	1

Table 2 shows an example of a feature vector extracted from AF IR video sequence T258, whose features are given in Table 1. This feature vector is used as input to a classifier that differentiates between the different classes of munitions' detonations. The feature vector extracted from visible camera video sequences and described in detail in other reports[2-4] allowed discrimination between each of the four classes of munitions' detonations. For the AF IR data, the feature vector allows events to be classified as HE airburst, HE point detonation, CB point detonation, or CB airburst. The mode of detonation (either airburst or point detonation of the CB munition), can be determined independently by acoustic sensors (triangulation of four sensors) as well as from the visible camera data. This further illustrates the importance of fusing information from different sensors.

Table 3 provides the feature vectors extracted from each of the available AF IR video sequences. The class provided in the right hand column of the table are either the known class (for the first 160 rounds) or the estimated class based on human review of the AF IR and DSI visible camera[2-4] video sequences. This table also presents (at the bottom) a few cases where the class was either unknown or where the IR camera did not capture the complete munition's detonation sequence (e.g., the detonation signature was cropped by the camera's field of view).

Table 3. Feature Vectors and Detonation Classes for AF IR Data Set

Test Name	Size1	Orientation	Eccentricity	Sequential	Class
chemair\T253	80	-17.16	0.64	1	CA
chemair\T255	89	-29.06	0.64	1	CA
chemair\T260	60	-24.85	0.69	1	CA
T173 (#18)	80	-52.39	0.75	1	CA
T175 (#18)	64	-53.8	0.71	0	CA
T181 (#18)	64	-27.82	0.585	0	CA
T242 (#20)	106	-51.73	0.695	1	CA
T244 (#20)	167	-54.87	0.83	1	CA
T246 (#20)	119	-52.05	0.685	1	CA
T251 (#21)	91	-62.21	0.275	1	CA
T252 (#21)	62	-40.02	0.575	0	CA
chemair\T257	38	-73.87	0.55	0	CA
chemair\T259	39	13.29	0.495	1	CA
T164 (#17)	27	-1.89	0.655	1	CA
T209 (#20)	68	12.86	0.57	0	CP
T215 (#20)	60	0	0.565	1	CP
T216 (#20)	47	-11.05	0.52	0	CP
T219 (#21)	81	-43.13	0.165	1	CP
T223 (#21)	7	0	0.76	1	CP
T225 (#21)	78	-14.76	0.53	1	CP
T227 (#22)	96	3.36	0.52	1	CP
T235 (#22)	70	-4.54	0.585	1	CP
T238 (#22)	35	-4.76	0.9	1	CP
chempoint\T114	291	10.14	0.38	1	CP
chempoint\T116	32	18.43	0.31	1	CP
chempoint\T127	152	0	0.47	1	CP
T163 (#17)	52	-10.29	0.58	1	CP
heair\T247	902	-30.17	0.575	1	HA
heair\T239	865	-49.83	0.505	1	HA
heair\T240	816	-34.97	0.68	1	HA
heair\T241	815	-33.34	0.505	1	HA
heair\T245	855	-41.01	0.525	1	HA
T168 (#17)	801	-44.45	0.515	1	HA
T171 (#18)	837	-37.07	0.57	1	HA
T176 (#18)	820	-51.45	0.475	1	HA
T179 (#18)	756	-29.14	0.52	1	HA
T185 (#18)	817	-36.88	0.54	1	HA
T249 (#21)	809	-40.51	0.545	1	HA
T250 (#21)	829	-32.77	0.555	1	HA
T256 (#21)	855	-45.11	0.475	1	HA
T258 (#21)	794	-42.47	0.545	1	HA
T222 (#21)	279	-0.89	0.82	1	HP
T174 (#18)	229	0.77	0.73	1	HP
T180 (#18)	174	-0.09	0.86	1	HP
T188 (#18)	159	-7.9	0.81	1	HP
T204 (#20)	310	3.42	0.785	1	HP
T208 (#20)	255	-2.99	0.775	1	HP
T210 (#20)	231	-2.13	0.83	1	HP
T211 (#20)	197	-12.39	0.8	1	HP
T212 (#20)	269	-3.38	0.85	1	HP
T214 (#20)	257	-4.82	0.795	1	HP
T217 (#21)	287	-2.54	0.815	1	HP
T218 (#21)	242	-2.71	0.805	1	HP
T221 (#21)	250	-2.06	0.855	1	HP
T224 (#21)	138	-5.93	0.76	1	HP
T228 (#22)	132	-1.81	0.9	1	HP
T233 (#22)	141	-2.27	0.88	1	HP
T236 (#22)	249	-1.86	0.9	1	HP
hepoint\T100	82	-5.92	0.72	1	HP
hepoint\T112	188	-5.44	0.65	1	HP
hepoint\T113	114	-7.41	0.825	1	HP
hepoint\T115	180	-0.99	0.7	1	HP
hepoint\T117	319	3.25	0.715	1	HP
hepoint\T123	70	-1.83	0.745	1	HP
hepoint\T125	177	-2.18	0.83	1	HP
hepoint\T129	197	-3.79	0.76	1	HP
hepoint\T131	213	-2.28	0.86	1	HP
T161	89	-3.77	0.89	1	HP
T232 (#22)	234	0.32	0.87	1	HP
T205 (#20)	126	-4.47	0.83	1	HP
T177 (#18)	80	-24.58	0.545	1	HP Offscreen
hepoint\T118	33	-63.3	0.34	1	HP Offscreen
T165 (#17)	143	-7.72	0.865	1	?
T234 (#22)	7	-14.68	0.85	0	?

This section provides figures and a discussion of how each of the individual features in Table 3 are used for discrimination. The figures show histograms of the feature values for each of the target classes (each target class is represented in a different color). Since the sequential feature is binary (a sequence is either sequential or not), a separate figure will not be generated for this feature. Instead, the data provided in Table 3 will be used to describe the importance of this feature in performing discrimination.

As previously mentioned, the size1 feature is the most important feature for performing discrimination when using the AF IR video data. Figure 8 provides a plot for the histograms for each target class for the size1 feature. The x axis is the feature value, and the y axis is the number of events with that particular feature value. Each target class is color coded. Magenta represents HE air munitions' detonations. Blue represents HE point detonations. Green represents CB point detonations, and red represents CB air detonations. A quick review of the data provided in Figure 8 clearly shows that the HE airbursts are fully separated from the other classes based solely on this one feature value. The importance of this feature in separating the other target classes is discussed in Figure 9 and the next paragraph.

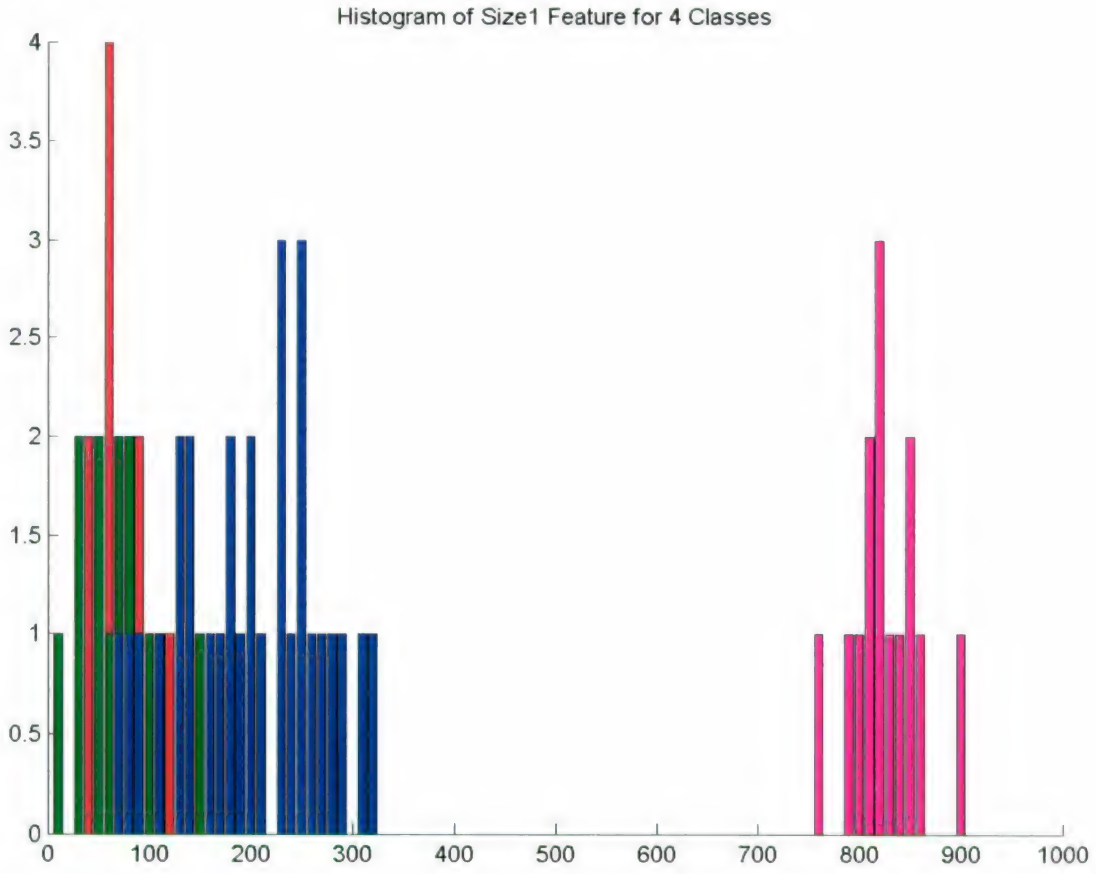

Figure 8. Size1 Feature Histograms for Four Classes of Munitions' Detonations

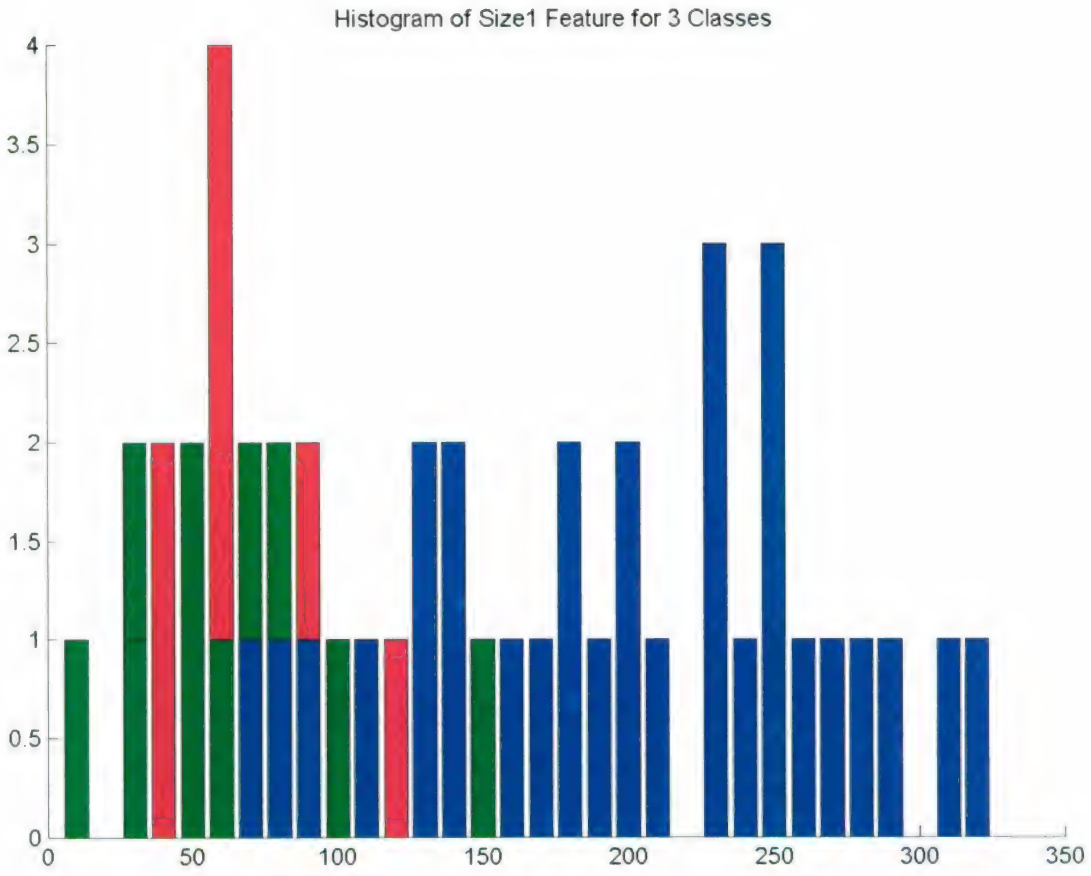

Figure 9. Size1 Feature Histograms for Three Classes of Munitions' Detonations

Figure 9 shows the size1 feature histograms for HE point, CB point, and CB air munitions' detonations. Again, the x axis is the size1 feature value, and the y axis is the number of events with the indicated feature value. The color coding is the same as that in Figure 8 (blue for HE point detonations, green for CB point detonations, and red for CB air detonations.) Figure 9 clearly shows three regions in the size1 feature space.

- Above a certain value of size1 (~160), all events are HE point detonation events (HE air detonations have the size1 values shown in Figure 8).

- Below a certain value of size1 (~60), all events are CB detonation events.

- Between these values there is a region with overlap between the CB detonation events and the HE point discharge events.

The classifier described in Section 4 exploits these observations. It separates the munitions' detonation classes using just this one feature where it can and uses other features when the size1 feature value is in the overlap region.

Histograms for the orientation feature are provided in Figure 10. Because the HE airbursts can be fully separated from the other classes just by using the size1 feature, the Orientation Feature histograms are provided for the HE point, CB point, and CB air detonations only. In Figure 10, blue represents HE point detonations, green represents CB point detonations, and red represents CB air detonations. The data in Figure 10 clearly show the ability to provide some separation of the CB airbursts (red) from the CB point detonations (green) and the HE point detonations (blue) using this feature. This observation is also used in the classifier described in Section 4.

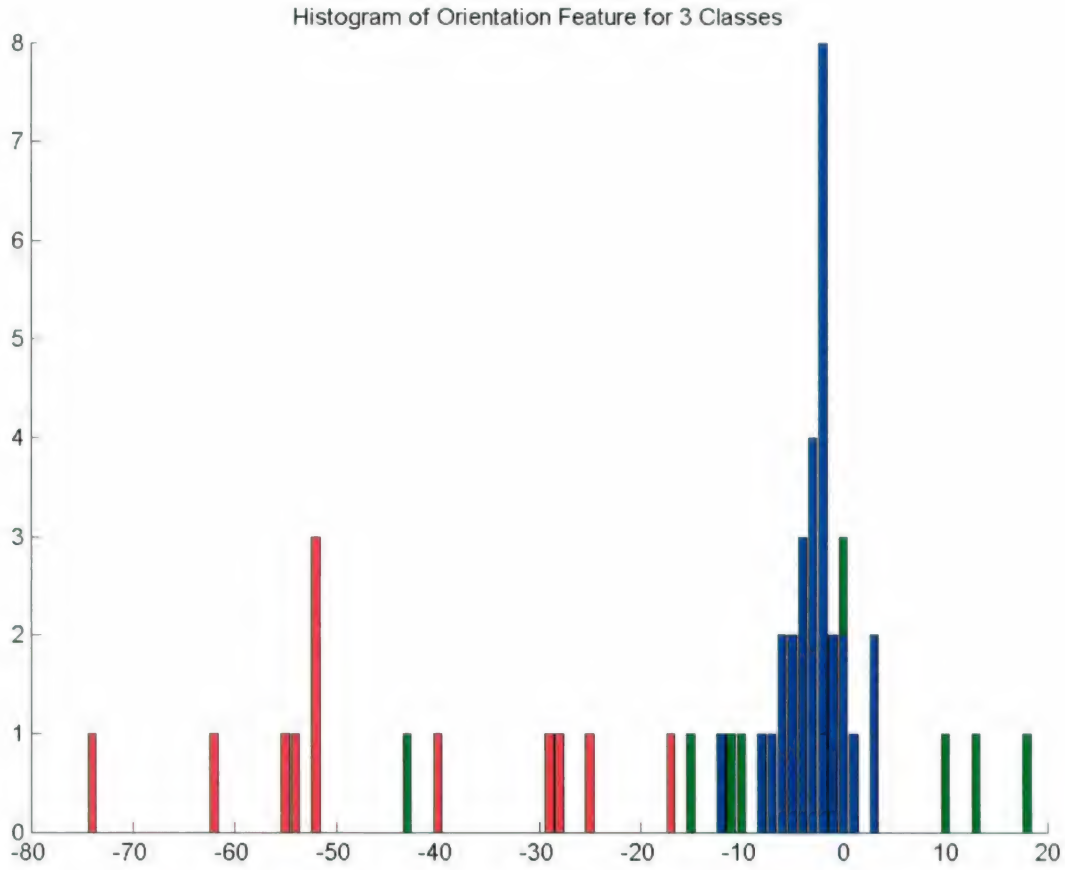

Figure 10. Orientation Feature Histograms for Three Classes of Munitions' Detonations

Figure 11 shows histograms for the eccentricity feature for the same three classes. Again, blue represents HE point detonations, green represents CB point detonations, and red represents CB airbursts. Figure 11 also shows the ability to separate the HE point detonation class from either the CB point or CB airburst classes using this feature. The classifier described in Section 4 also exploits this observation.

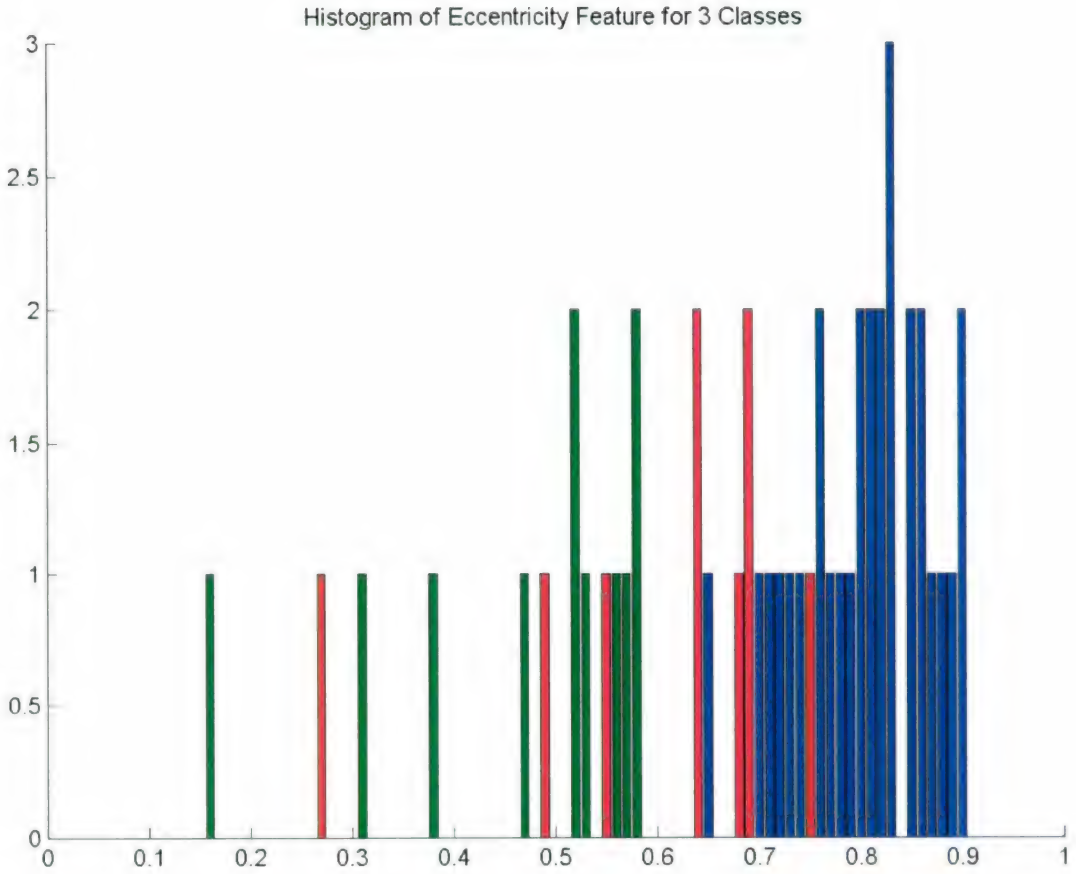

Figure 11. Eccentricity Feature Histograms for Three Classes of Munitions' Detonations

Histograms for the sequential feature are not generated as this is a binary feature. However, the information provided in Table 3 can be used to determine the value of this feature in performing discrimination. In every case evaluated, the triggering was sequential for the HE air and HE point munitions' detonations. In 6 cases out of 27, CB munitions' detonations were not sequential. The classifier described in Section 4 also exploits this observation.

4. CLASSIFIER DESCRIPTIONS AND RESULTS

The Linguistic-Fuzzy Classifier approach previously described in detail[4] was used to evaluate the feature vector and to generate confidence values for discrimination. In this case, we have developed a hierarchical classifier that first tries to use the size1 feature alone for performing classification.

The following descriptions are used for the target classes:

- **HE air detonations** have ***very large size1*** values
- **HE point detonations** have ***large size1*** values
- **CB detonations** have ***small size1*** values
- **Detonations where we need more information** occur over an ***in-between range of size1*** values.

Figure 12 shows size1 feature values and membership functions for all four classes of munitions' detonations. Figure 13 shows the size1 feature histograms and membership functions for the region where there is more class overlap. In both figures, the blue histograms represent the HE munitions (both point and air), and the red histograms represent the CB munitions. The green membership function defines ***very large size1*** feature values in the class descriptions above (only shown in Figure 12). The yellow membership function defines ***large size1*** feature values, and the magenta membership function defines ***small size1*** feature values in the class descriptions above. Lastly, the cyan membership function defines the ***in-between range of size1*** in the class descriptions above.

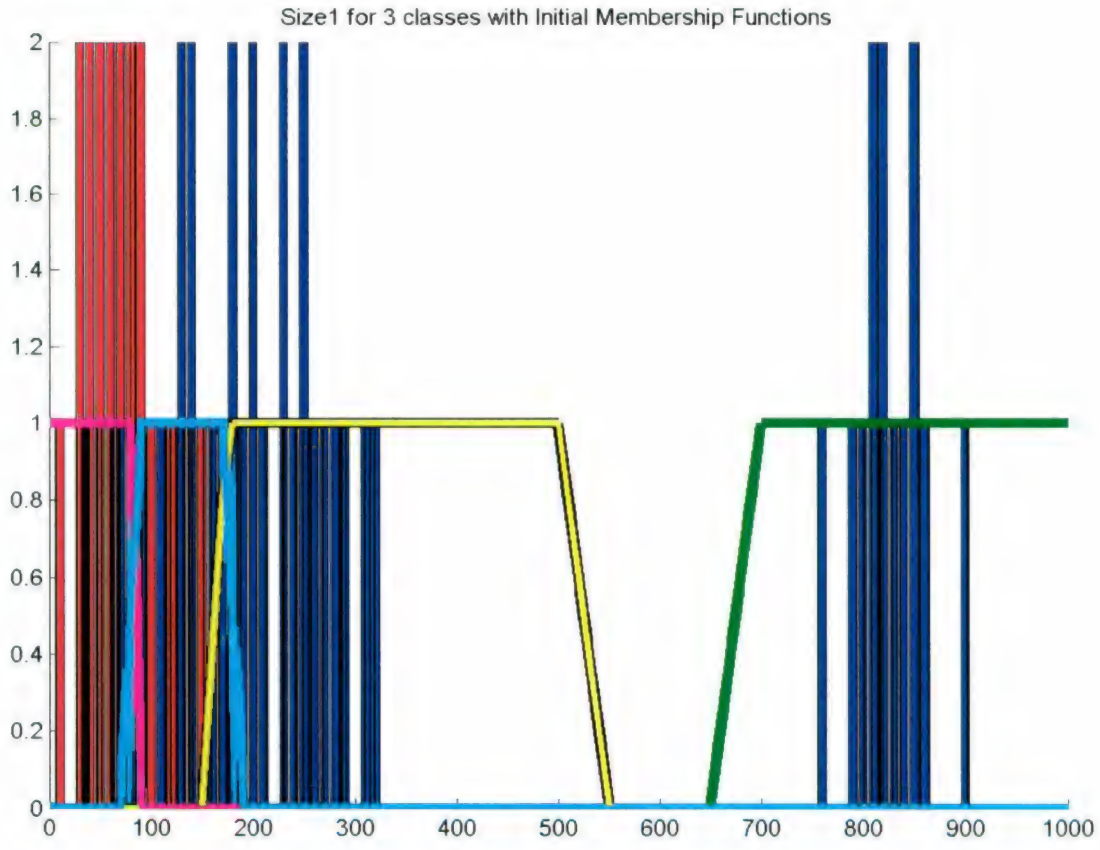

Figure 12. Histograms and Membership Functions for the Size1 Feature

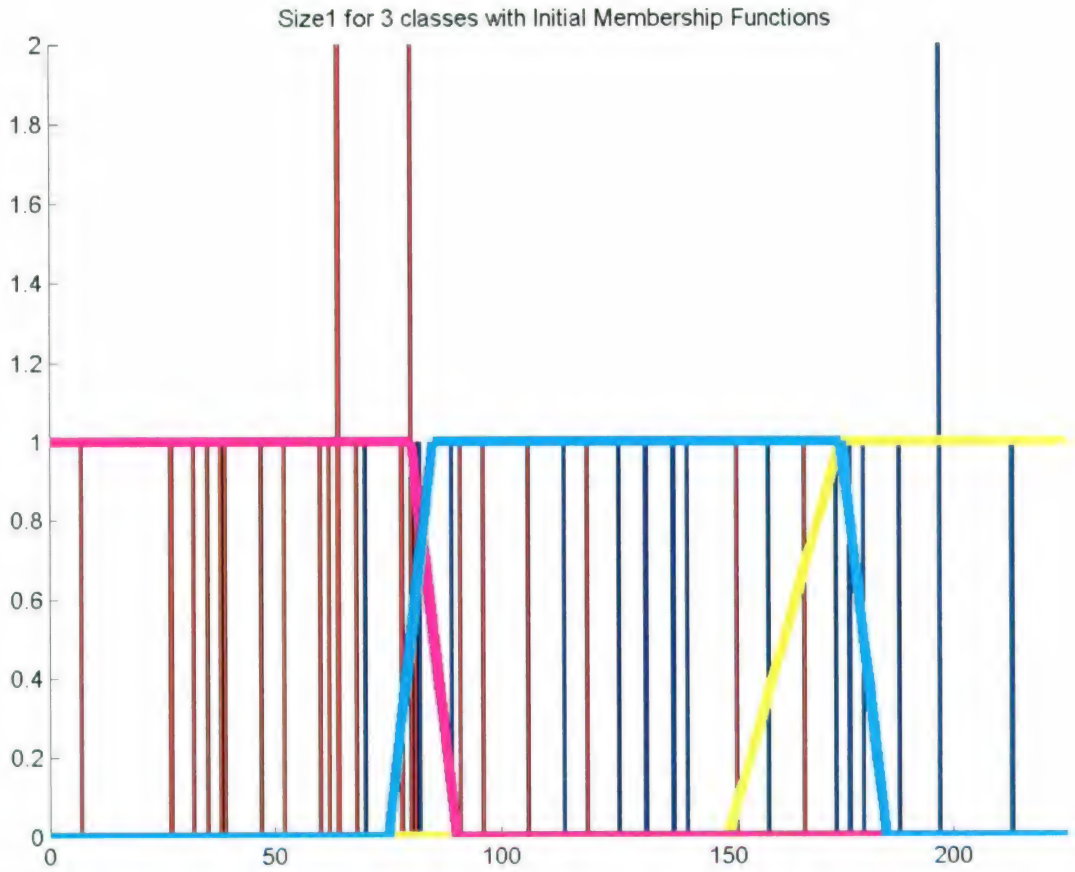

Figure 13. Histograms and Membership Functions for the Size1 Feature (Expanded Scale)

To generate confidence values using the size1 feature value, we first determine to which membership function the particular value of the size1 feature belongs and use this to generate the confidence value. For example, if the size1 feature value is 800, than the intersection with the ***very large size1*** membership function is 1, and the intersection with all other membership functions is zero (Figure 12). This results in a 100% confidence value that this is an **HE air detonation**. Similarly, a size1 value of 30 results in an intersection of 1 with the ***small size1*** membership function and an intersection of zero with all other membership functions.

Consequently, this results in a 100% confidence value that this is a **CB detonation**. Finally, if the size1 feature value is 160, we have an intersection of approximately 0.3 with the ***large size1*** membership function and an intersection of 1 with the ***in-between range of size1*** membership function. In this case, we would classify the event as a **detonation where we need more information**, and other features would be evaluated by different linguistic-fuzzy classifiers to generate a confidence value that would be used for discrimination. In cases where the size1 feature value results in confidence values being generated for **CB detonation, detonation where we need more information,** or **HE point detonation,** the higher confidence value is used to determine the classification path. In cases where either the **CB detonation** or

HE point detonation confidences are either greater than or equal to the **detonation where we need more information** confidence value, either the **CB** or **HE point detonation** confidence value is used as the final output for the classifier. In cases where the **detonation where we need more information** confidence value is greater than either the **CB** or **HE point detonation** confidences, the next layer of the classifier (described below) is used to generate the final output for the classifier.

For these interim cases, we use the following descriptions of the target classes:

- **HE point detonations** have ***higher size1*** values, ***higher eccentricity*** values, and ***near-zero orientations.***

- **CB detonations** have ***lower size1*** values, ***lower eccentricity*** values, ***more negative orientation*** values, and are not always ***sequential.***

Figure 14 shows the histograms and membership functions used in this layer of the classifier (excluding the sequential feature - its importance was described in Section 3.)

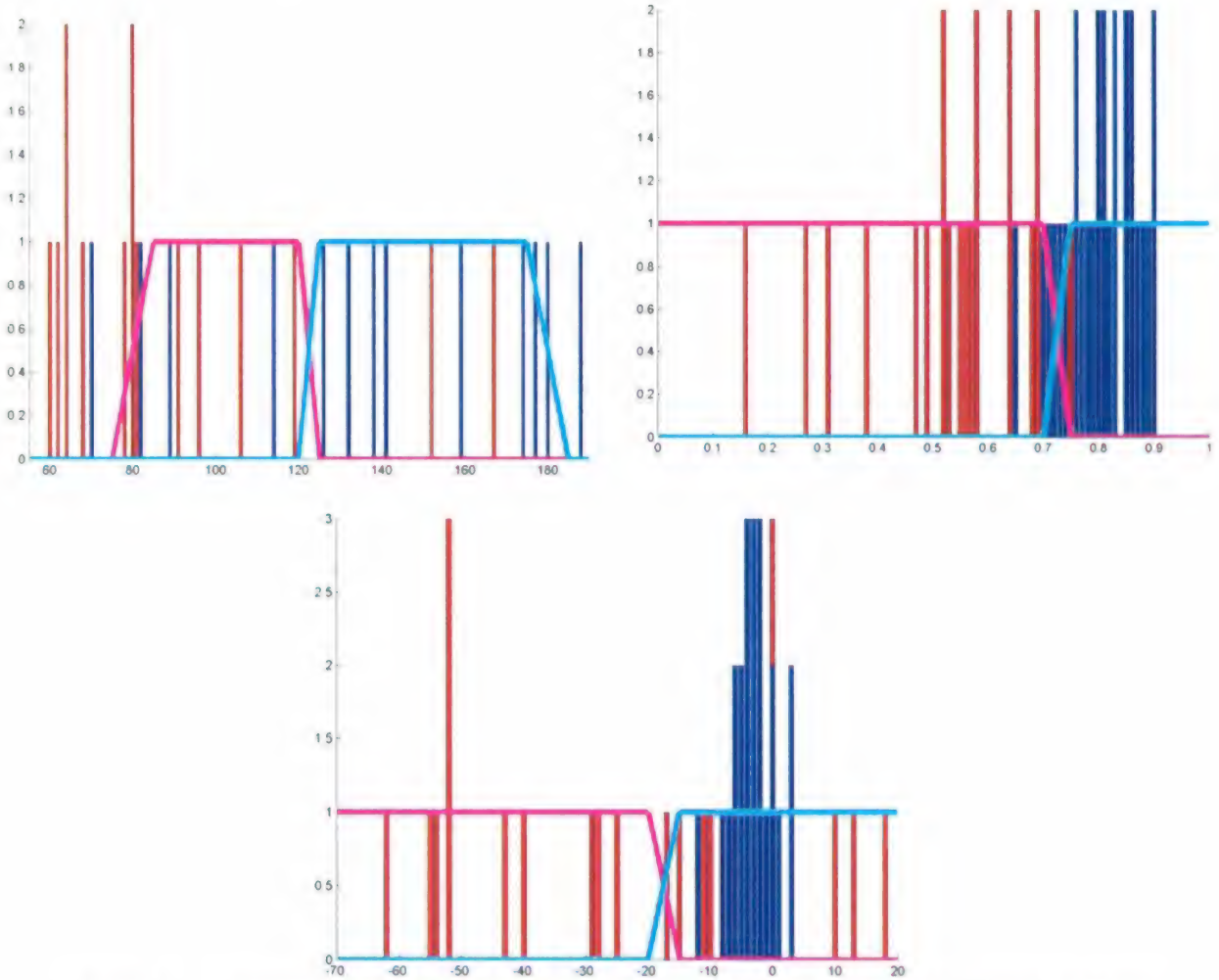

Figure 14. Histograms and Membership Functions Used in the Second Classifier Layer

In Figure 14, the plot on the upper left is for the size1 feature. The plot on the upper right is for the eccentricity feature, and the plot in the lower center is for the orientation feature. In these plots, the blue histograms represent HE point detonations, and the red histograms represent CB point and air detonations. The membership functions shown for the size1 feature cover the same range as the ***in-between range of size1*** membership function described earlier in Figure 13. The magenta membership function defines ***lower size1*** in the class descriptions provided above, while the cyan membership function defines ***higher size1*** in the class descriptions. The magenta membership function in the eccentricity feature space defines ***lower eccentricity,*** while the cyan membership function defines ***higher eccentricity***. The magenta membership function in the orientation space defines ***more negative orientation,*** while the cyan membership function defines ***near-zero orientation***.

It is important to keep in mind that the second layer of the classifier is only used in cases where a class declaration cannot be made based on the first layer of the classifiers' assessment of size1 feature value (i.e., when size1 is neither too high nor too low, but falls in the mid range). This second layer classifier is used in < 30% of the cases that were evaluated. A review of the histograms and membership functions provided in Figure 14 shows that the classes cannot be easily separated using the single features and membership functions shown in the figure. For example, the CB and HE point detonations have orientations that are in the same range of angles (near zero). This becomes apparent when the data previously presented in Figure 10 is considered with that provided in Figure 14. Consequently, this feature is more valuable in separating the CB air detonations from the HE point detonations (as well as from the CB point detonations). As a second example, a review of the eccentricity feature values and membership functions shows that this feature is more useful in separating the CB point detonations from the HE point detonations. But, the feature is less useful in separating CB air detonations from HE point detonations. This becomes apparent when the data previously presented in Figure 11 is considered with that provided in Figure 14. There is better separation between the CB (point and air) detonations and the HE point detonations with the size1 feature data shown in Figure 14. However, there is still some overlap between the classes (considering the membership functions shown in Figure 14) in this feature space. As previously mentioned in this report, 6 of the 27 CB detonation (and 0 of 44 HE detonation) sequences evaluated produced nonsequential triggering of the detector. Again, this feature can contribute towards confidence estimation, but it should not independently drive the final class declaration.

Since there is only fair separation between the classes using single features in this second layer classifier, it is a good opportunity to demonstrate the value of data (or feature) fusion to achieve better discrimination between the classes. We use the Linguistic-Fuzzy Classifier[4] for that purpose. We configured the linguistic-fuzzy classifier in a manner that requires at least two of the three major attributes to have a strong membership in the appropriate membership functions to drive the confidence value to a level higher than 0.5. This is accomplished through the proper selection of weights for each of the attributes used in the classifier. The sequential feature is a less important attribute for discrimination. Therefore, for this feature, a weight was selected that results in only a small increase (approximately 0.08) in confidence value for CB detonations when the video sequence results in the detector triggering in a nonsequential manner.

Using these considerations as guide, the following relationship is used to estimate a confidence value for HE point detonations:

$$CONF_{HEpoint} = (W_{higher\ size1} * Mem(\textbf{\textit{higher size1}}))^2 + (W_{higher\ eccentricity} * Mem(\textbf{\textit{higher eccentricity}}))^2 + (W_{orientation\ near\ zero} * Mem(\textbf{\textit{orientation near zero}}))^2 / (W_{higher\ size1}^2 + W_{higher\ eccentricity}^2 + W_{orientation\ near\ zero}^2) \quad (1)$$

where

$CONF_{HEpoint}$ = confidence that the observed detonation is an HE point munition's detonation - maximum value is 1 (100% confidence) and minimum value is 0 (0% confidence)

$W_{higher\ size1}$ = weight for the size1 feature for performing HE detonation discrimination = 0.5

$W_{higher\ eccentricity}$ = weight for the eccentricity feature for performing HE detonation discrimination = 0.5

$W_{orientation\ near\ zero}$ = weight for the orientation feature for performing HE detonation discrimination = 0.5

Mem(***higher size1***) = membership of the size1 feature value in the ***higher size1*** membership function shown in Figure 14

Mem(***higher eccentricity***) = membership of the eccentricity feature value in the ***higher eccentricity*** membership function shown in Figure 14

Mem(***orientation near zero***) = membership of the orientation feature value in the ***orientation near zero*** membership function shown in Figure 14

The membership functions used in this classifier were selected based on analyses of the histograms provided in Figure 14. The weights for the individual features were selected based on the considerations discussed earlier in this report.

The following relationship is used to estimate a confidence value for CB detonations:

$$CONF_{CB} = (W_{lower\ size1} * Mem(\textbf{\textit{lower size1}}))^2 + (W_{lower\ eccentricity} * Mem(\textbf{\textit{lower eccentricity}}))^2 + (W_{more\ negative\ orientation} * Mem(\textbf{\textit{more negative orientation}}))^2 + (W_{not\ sequential} * Mem(\textbf{\textit{not sequential}}))^2 / (W_{lower\ size1}^2 + W_{lower\ eccentricity}^2 + W_{more\ negative\ orientation}^2 + W_{not\ sequential}^2) \quad (2)$$

where

$CONF_{CB}$ = confidence that the observed detonation is a CB munition's detonation (point or airburst) - maximum value is 1 (100% confidence) and minimum value is 0 (0% confidence)

$W_{lower\ size1}$	= weight for the size1 feature for performing CB detonation discrimination = 0.5
$W_{lower\ eccentricity}$	= weight for the eccentricity feature for performing CB detonation discrimination = 0.5
$W_{not\ sequential}$	= weight for the eccentricity feature for performing CB detonation discrimination = 0.25
Mem(***lower size1***)	= membership of the size1 feature value in the ***lower size1*** membership function shown in Figure 14
Mem(***lower eccentricity***)	= membership of the eccentricity feature value in the ***higher eccentricity*** membership function shown in Figure 14
Mem(***more negative orientation***)	= membership of the orientation feature value in the ***more negative orientation*** membership function shown in Figure 14
Mem(***not sequential***)	= 1 if the detector triggered not sequentially on the video sequence (i.e., the sequential feature is = 0) or = 0 if the detector triggered sequentially

As in the case described earlier, the membership functions used in this classifier resulted from analyses performed on the histograms provided in Figure 14. The weights were selected for the reasons previously discussed in detail in this section of the report.

Section 5 will provide the results obtained using the classifiers described in this section.

5. LINGUISTIC-FUZZY CLASSIFIER RESULTS SUMMARY

Table 4 gives the results of applying the detector, feature extraction, and linguistic-fuzzy classifiers to each of the available AF IR DSI video sequences. The table also provides the file name, the feature vector (size1, orientation, eccentricity, and sequential status), the linguistic-fuzzy classifier confidence values for HE air detonation, HE point detonation and CB detonation, the final class declaration, and a comment field. The final class declarations are based on the confidence values provided in this table. The highest confidence value of the three outputs from the linguistic-fuzzy classifier determines the final class declaration. When the two highest confidence values were within 0.1 of each other, that event would be declared indeterminate based on the classifier outputs (note this did not happen with any of the feature vectors extracted from the 74 AF IR video sequences).

Table 4. Linguistic-Fuzzy Classifier AF IR Results Summary

Test Name	Size1	Orientation	Eccentricity	Sequential	HE Air Conf	HE Point Conf	CB Conf	Class	Comments
chemair\T253	80	-17.16	0.64	1	0	0	1	CB	
chemair\T255	89	-29.06	0.64	1	0	0	0.96	CB	
chemair\T260	60	-24.85	0.69	1	0	0	1	CB	
T173 (#18)	80	-52.39	0.75	1	0	0	1	CB	
T175 (#18)	64	-53.8	0.71	0	0	0	1	CB	
T181 (#18)	64	-27.82	0.585	0	0	0	1	CB	
T242 (#20)	106	-51.73	0.695	1	0	0	0.96	CB	
T244 (#20)	167	-54.87	0.83	1	0	0.82	0.55	HP (CB)	Event Obscured by Reticule
T246 (#20)	119	-52.05	0.685	1	0	0	0.96	CB	
T251 (#21)	91	-62.21	0.275	1	0	0	0.96	CB	
T252 (#21)	62	-40.02	0.575	0	0	0	1	CB	
chemair\T257	38	-73.87	0.55	0	0	0	1	CB	
chemair\T259	39	13.29	0.495	1	0	0	1	CB	
T164 (#17)	27	-1.89	0.655	1	0	0	1	CB	
T209 (#20)	68	12.86	0.57	0	0	0	1	CB	
T215 (#20)	60	0	0.565	1	0	0	1	CB	
T216 (#20)	47	-11.05	0.52	0	0	0.58	0.83	CB	
T219 (#21)	81	-43.13	0.165	1	0	0	0.9	CB	
T223 (#21)	7	0	0.76	1	0	0	1	CB	
T225 (#21)	78	-14.76	0.53	1	0	0	1	CB	
T227 (#22)	96	3.36	0.52	1	0	0.58	0.78	CB	
T235 (#22)	70	-4.54	0.585	1	0	0	1	CB	
T238 (#22)	35	-4.76	0.9	1	0	0	1	CB	
chempoint\T114	291	10.14	0.38	1	0	1	0	HP (CB)	False Negative
chempoint\T116	32	18.43	0.31	1	0	0	1	CB	
chempoint\T127	152	0	0.47	1	0	0.82	0.55	HP(CB)	False Negative
T163 (#17)	52	-10.29	0.58	1	0	0	1	CB	
heair\T247	902	-30.17	0.575	1	1	0	0	HA	
heair\T239	865	-49.83	0.505	1	1	0	0	HA	
heair\T240	816	-34.97	0.68	1	1	0	0	HA	
heair\T241	815	-33.34	0.505	1	1	0	0	HA	
heair\T245	855	-41.01	0.525	1	1	0	0	HA	
T168 (#17)	801	-44.45	0.515	1	1	0	0	HA	
T171 (#18)	837	-37.07	0.57	1	1	0	0	HA	
T176 (#18)	820	-51.45	0.475	1	1	0	0	HA	
T179 (#18)	756	-29.14	0.52	1	1	0	0	HA	
T185 (#18)	817	-36.88	0.54	1	1	0	0	HA	
T249 (#21)	809	-40.51	0.545	1	1	0	0	HA	
T250 (#21)	829	-32.77	0.555	1	1	0	0	HA	
T256 (#21)	855	-45.11	0.475	1	1	0	0	HA	
T258 (#21)	794	-42.47	0.545	1	1	0	0	HA	
T222 (#21)	279	-0.89	0.82	1	0	1	0	HP	
T174 (#18)	229	0.77	0.73	1	0	1	0	HP	
T180 (#18)	174	-0.09	0.86	1	0	1	0	HP	
T188 (#18)	159	-7.9	0.81	1	0	1	0	HP	
T204 (#20)	310	3.42	0.785	1	0	1	0	HP	
T208 (#20)	255	-2.99	0.775	1	0	1	0	HP	
T210 (#20)	231	-2.13	0.83	1	0	1	0	HP	
T211 (#20)	197	-12.39	0.8	1	0	1	0	HP	
T212 (#20)	269	-3.38	0.85	1	0	1	0	HP	
T214 (#20)	257	-4.82	0.795	1	0	1	0	HP	
T217 (#21)	287	-2.54	0.815	1	0	1	0	HP	
T218 (#21)	242	-2.71	0.805	1	0	1	0	HP	
T221 (#21)	250	-2.06	0.855	1	0	1	0	HP	
T224 (#21)	138	-5.93	0.76	1	0	1	0	HP	
T228 (#22)	132	-1.81	0.9	1	0	1	0	HP	
T233 (#22)	141	-2.27	0.88	1	0	1	0	HP	
T236 (#22)	249	-1.86	0.9	1	0	1	0	HP	
hepoint\T100	82	-5.92	0.72	1	0	0	0.8	CB (HP)	False Positive
hepoint\T112	188	-5.44	0.65	1	0	1	0	HP	
hepoint\T113	114	-7.41	0.825	1	0	0.82	0.55	HP	
hepoint\T115	180	-0.99	0.7	1	0	1	0	HP	
hepoint\T117	319	3.25	0.715	1	0	1	0	HP	
hepoint\T123	70	-1.83	0.745	1	0	0	1	CB (HP)	False Positive
hepoint\T125	177	-2.18	0.83	1	0	1	0	HP	
hepoint\T129	197	-3.79	0.76	1	0	1	0	HP	
hepoint\T131	213	-2.28	0.86	1	0	1	0	HP	
T161	89	-3.77	0.89	1	0	0.82	0.55	HP	
T232 (#22)	234	0.32	0.87	1	0	1	0	HP	
T205 (#20)	126	-4.47	0.83	1	0	1	0	HP	
T177 (#18)	80	-24.58	0.545	1	0	0	1	CB (HP)	HP Edge of FOV
hepoint\T118	33	-63.3	0.34	1	0	0	1	CB (HP)	HP Edge of FOV
T165 (#17)	143	-7.72	0.865	1	0	1	0	HP	
T234 (#22)	7	-14.68	0.85	0	0	0	1	CB	

Overall, excellent discrimination results have been obtained using the feature vectors and linguistic-fuzzy classifiers described herein. Considering the results from all 74 video sequences, the linguistic-fuzzy classifiers correctly classified the detonation events 91% of the time. Three CB detonation events were declared HE point detonations (false negatives), and four HE point detonations were declared CB detonations (false positives).

Please note that in two HE point detonation events, the detonation signatures were at the very edge of the field of view of the camera and that the feature values for size1 and eccentricity were corrupted since the signature in the image was cropped. Specifically, this caused these two events to be declared CB detonations. The two events are noted in Table 4. In addition, one of the CB airburst detonation's signature was corrupted by video overlay reticule. This corrupted the eccentricity feature value and drove the declaration of this video sequence to HE point detonation. If the three events were eliminated, the linguistic fuzzy classifier correctly classified detonations in 94% of the cases with two false positives and two false negatives. These results clearly demonstrate the feasibility of using IR imaging systems to detect CB munitions' use. In addition, this discrimination can occur well within 1 s of a munition's detonation (including feature extraction, feature evaluation, and final event type declaration).

A secondary benefit of the linguistic-fuzzy classifiers described in this report is that the confidence levels (as well as either some or all of the features used to generate the confidence values) can be used as input to a multisensor data fusion engine. For example, the confidence values and either some or all of the feature values provided in Table 4 could be combined with the confidence values and either some or all of the feature values extracted from a visible camera video sequences.[4] This will be the topic of a future report. Also, confidence and feature values from the imaging systems (IR and visible) can also be combined with those obtained using acoustic and seismic sensors that are also part of the DSI sensor suite. This also will be the topic of a future report because it is likely that it will increase the accuracy of the CB detection/early warning process.

6. CONCLUSIONS

In this report, we describe the methods used to identify frames of interest and to extract features from the Disparate Sensor Integration (DSI) Air Force (AF) IR Video Sequences. We also describe how the features extracted from individual frames are combined to create a single feature vector. These processes are completed in the first 10 video frames (0.33 s) after a munition's detonation event is first detected. We also describe a unique classifier system that we used to evaluate the feature vectors and to develop confidence values for HE air detonations, HE point detonations, and CB detonations. We show how we can use these confidence values to detect CB munitions' use.

When we apply these methods to the DSI AF IR video data set, we achieved a very high success rate in identifying CB munitions. If we consider video sequences where the detonation signatures are not corrupted by video artifacts (cropping), we were able to correctly identify the munition's fill (either CB or HE) in 94% of the cases evaluated. In the 71 video

sequences evaluated, there were two false positives and two false negatives. These results clearly demonstrate the potential for detecting CB rounds using IR imaging systems. In addition, the methods used will allow discrimination to occur well within 1 s of a munition's detonation.

Future work will be directed at fusing the DSI AF IR imaging system results with visible imaging system results. The DSI Dugway Proving Ground (DPG) visible imaging system confidence outputs and features' vectors are described in detail.[4] This work will use the confidence values and either some or all of the feature values (described herein and in Reference 4) as inputs to a multisensor data fusion engine. We anticipate that further improvements in classification results will be obtained when this next level of data fusion is performed.

Future work will also be directed at fusing the results obtained with the visible and IR imaging systems with those obtained using the DSI acoustic and seismic sensors. As these sensors provide a more orthogonal detection modality, we anticipate that performing multisensor data fusion at this level will have significant pay offs in classification results and robustness of final target declarations. We have also initiated a modeling and simulation effort that will be used to predict performance of a DSI sensor suite in more complex simulated measurement environments. The simulated environments include scenarios where the detonation events occur at multiple locations with respect to the sensor locations as well as environments where multiple detonation events occur nearly simultaneously. The modeling efforts will also be used to help define the robustness of individual classifiers at the sensor levels as well as fusing different sensor types. Through simulation, we will be able to demonstrate the many benefits that are likely to be obtained through performing multisensor data fusion.

The methods described herein provide a computationally efficient and robust means for detection and early warning when CB munitions are used.

LITERATURE CITED

1. Birenzvige, A.; Sickenberger, D.; Reyes, F. *Disparate Sensor Integration Program Description and Preliminary Data Analysis*; ECBC-TR-251; U.S. Army Edgewood Chemical Biological Center: Aberdeen Proving Ground, MD, 2002; UNCLASSIFIED Report (AD-B284 556).

2. Nelson, B.; Birenzvige, A.; Underwood, W. *Evaluation of an Optical Imager as a Detector for Chemical Munitions*; ECBC-TR-308; U.S. Army Edgewood Chemical Biological Center: Aberdeen Proving Ground, MD, 2003; UNCLASSIFIED Report (AD-B293 345).

3. Nelson, B.; Birenzvige, A.; Underwood, W.; Sickenberger, D. *CB Round Discrimination Fusing Visible and IR Camera Data.* Presented at the 2003 SPIE Conference, Orlando, FL, Volume 5099, pp 397-408, 2003.

4. Nelson, B.; Birenzvige, A. *Linguistic-Fuzzy Classifier for Discrimination and Confidence Value Estimation*; ECBC-TR-353; U.S. Army Edgewood Chemical Biological Center: Aberdeen Proving Ground, MD, 2004; UNCLASSIFIED Report.